AMERICAN METEOROLOGICAL SOCIETY

Journal of Hydrometeorology

EARLY ONLINE RELEASE

The DOI for this manuscript is doi: 10.1175/JHM-D-14-0094.1

Effects of Increasing Horizontal Resolution in a Convection Permitting Model on Flood Forecasting: The 2011 Dramatic Events in Liguria (Italy)

Silvio Davolio
Institute of Atmospheric Sciences and Climate, National Research Council, CNR ISAC, Bologna, Italy

Francesco Silvestro
CIMA Research Foundation, Savona, Italy

Piero Malguzzi
Institute of Atmospheric Sciences and Climate, National Research Council, CNR ISAC, Bologna, Italy

Corresponding author address: Silvio Davolio, Institute of Atmospheric Sciences and Climate, National Research Council (CNR ISAC), Via Gobetti 101, 40129 Bologna, Italy.
E-mail: s.davolio@isac.cnr.it

Abstract

Coupling meteorological and hydrological models is a common and standard practice in the field of flood forecasting. In this study, a Numerical Weather Prediction (NWP) chain based on BOLAM and MOLOCH models was coupled with the operational hydrological forecasting chain of the Liguria Hydro-Meteorological Functional Centre to simulate two major floods that occurred during autumn 2011 in Northern Italy. Different atmospheric simulations were performed by varying the grid spacing (between 1 and 3 km) of the high-resolution meteorological model and the set of initial/boundary conditions driving the NWP chain. The aim was to investigate the impact of these parameters not only from a meteorological perspective, but also in terms of discharge predictions for the two flood events. The operational flood forecasting system was thus used as a tool to validate in a more pragmatic sense the quantitative precipitation forecast obtained from different configurations of the NWP system. The results showed an improvement in flood prediction when a high-resolution grid was employed for atmospheric simulations. In turn, a better description of the evolution of the precipitating convective systems was beneficial for the hydrological prediction. Although the simulations underestimated the severity of both floods, the higher resolution model chain would have provided useful information to the decision makers in charge of protecting citizens.

1. Introduction

Heavy precipitation and floods can be dangerous and costly natural hazards in the Mediterranean basin, causing casualties and remarkable damages. Several international research programs (e.g. HyMeX, Drobinski et al. 2014) have recently sought to improve the understanding, monitoring, and modeling of these phenomena in order to prevent or reduce the associated damages to society and to the environment. Liguria, a coastal region in Northern Italy, presents characteristics typical of the Mediterranean area, being a narrow strip of land separating the Alps and Apennines from the sea. The steep and complex orography reaches high elevations (around 2000 meters) within a few kilometers of the coast, and a number of small catchments (only a few are larger than 200 km^2), characterized by a response time of a few hours at most, have their outlets in the Mediterranean Sea. Due to the topography, most of the urban areas are along the coast, often in proximity to a river outlet. Therefore, a severe weather event represents a serious threat for Liguria, where heavy and persistent rainfall can become a devastating flood in few hours. For these reasons, Liguria was selected and investigated as a hydro-meteorological site of interest during the HyMeX field campaign (SOP1, Ducrocq et al. 2014, Ferretti et al. 2014) that took place in autumn 2012.

The meteorological conditions conducive to heavy rainfall are met most often during autumn, when large-scale synoptic disturbances propagate and deepen in the Mediterranean basin. The Mediterranean Sea acts as a reservoir of humidity and heat, feeding low-level jets that convey moisture towards the Ligurian coastal slopes exposed to southerly flows. These conditions were indeed associated with two devastating flood episodes that occurred in fall 2011, on 25 October (“Cinque Terre” event, hereafter

referred to as CT) and 04 November ("Genoa" event, hereafter referred to as GE). In addition to the relevant differences shown at the mesoscale, both cases were characterized by the presence of intense, localized, and stationary convective activity that was responsible for the exceptional amount of precipitation that fell in less than one day. The CT and GE events caused thirteen and six casualties respectively, with relevant damage to infrastructure, buildings, and private and public properties estimated in the tens of millions of euros (Silvestro et al., 2012).

Several recent studies investigated these episodes from different perspectives. Rebora et al. (2013) provided a detailed and comprehensive meteorological overview of both events and identified some key ingredients underlying severe rainfall episodes using the available monitoring platforms. Silvestro et al. (2012) presented the hydrological aspects, analyzing the operational output available in real time at the Hydro-Meteorological Functional Centre (HMFC) of the Liguria Region in charge of issuing forecasts and alerts for civil protection purposes. Finally, two modeling studies (Fiori et al. 2014; Buzzi et al. 2014) were devoted to the identification of the key numerical aspects impacting on the ability to perform quantitative precipitation forecasting (QPF). In particular, the latter study further investigated the main dynamical mechanisms responsible for the triggering, development, and propagation of the precipitating systems, highlighting the combined effect of mesoscale forcing and orographic lifting in the two events.

Buzzi et al. (2014) also evaluated the performance of a convection-permitting model (MOLOCH, described in Sec. 2a) at various horizontal resolutions (between 1 and 3 km), driven by different global model datasets. Realistic simulations, in terms of total

accumulated precipitation, were obtained only for short-term forecasts (in agreement with Fiori et al. 2014), using grid spacing small enough to properly reproduce the small-scale features (low-level convergence and orographic lifting) that determined the onset of convection. Although the evaluation was mainly qualitative, it did show that increasing model's horizontal resolution improved both the forecast of precipitation amounts and geographical localization.

The goal of this study was to provide a quantitative evaluation of these simulation results in a pragmatic framework. Thus, instead of computing classical skill scores, the effect of different horizontal resolutions and initial/boundary conditions on QPF was evaluated in term of discharge predictions, applying MOLOCH output to the hydro-meteorological chain in operation at the time of the events at the HMFC (see Sec. 2b). This is an approach commonly employed by hydrologists interested in evaluating Numerical Weather Prediction (NWP) models (Cuo et al. 2011), who can then use their own sets of operationally available measurements. The objective is to verify if the meteorological improvements "propagate" into the hydrological prediction. In other words, the hydrological chain is used to quantitatively validate the QPF.

It is not obvious, however, whether an improved meteorological forecast corresponds to an improved forecast of hydrological response, since the relevant scales of validation for hydrology, the individual river's catchments, are remarkably smaller than the meteorological scales of validation (Pappenberger et al. 2008). Along this line, coupling meteorological and hydrological models is a common practice for streamflow forecasting that can be used for a practical evaluation of the QPF (Westrick and Mass 2001; Roberts et al. 2009; Ghile and Schulze 2010). At variance with previous studies

that found a general improvement with decreasing grid spacing, the present study specifically focuses on very high-resolution (between 1 and 3 km grid spacing) meteorological forecasts dealing with simulations of convective phenomena, which are associated with small-scale processes and limited intrinsic predictability (Hohenegger and Schär 2007).

High horizontal resolution is not only necessary to properly describe convective system dynamics and orographic forcing, but also recommended in deterministic operational practice (Cuo et al. 2010). Ensemble procedures are becoming an established research and operational field (Cloke and Pappenberger 2009) even for mesoscale meteorological models and short lead times below 24 hours, such as those considered here (which are in between very-short and short-range - WMO 1992). However, an appropriate rainfall downscaling procedure (see Sec. 2b) based on a meteorological deterministic approach (Fundel et al. 2010) may still help fill the gap between meteorological output and required hydrological input, taking into account the uncertainty related to the spatial-temporal variability of the rainfall fields at scales shorter than those at which QPF is reliable (Siccardi et al. 2000; Silvestro et al. 2011).

The paper is organized as follows. Section 2 describes the modeling chains and methods. Section 3 reports a brief description of the two heavy rainfall episodes and the discussion of the results from the meteorological perspective. Section 4 presents, more extensively, the hydrological perspective. Summary and conclusions are reported in Section 5.

2. Methods

a. The Numerical Weather Prediction System

Two different mesoscale models are employed in succession for the hindcast experiments: BOLAM and MOLOCH. These NWP models were developed at the Institute of Atmospheric Sciences and Climate of the Italian National Research Council (CNR – ISAC) and constitute its operational meteorological chain (http://www.isac.cnr.it/dinamica/projects/forecasts). The BOLAM model – for a description refer to Buzzi et al. (2003) and Davolio and Buzzi (2004) – is a limited-area hydrostatic model based on primitive equations with a convective parameterization based on Kain (2004). The BOLAM model is employed to provide the lateral boundary conditions for MOLOCH at hourly frequency. This current practice has proved to be reliable and economical in bridging the gap between the coarse spatial (0.5 degrees for the NOAA-GFS data and about 0.20 degrees for the ECMWF-IFS data) and temporal (3 hours) resolution of global model fields and the high-resolution forecasts. Since the results presented in the following are based on MOLOCH simulations, only a detailed description of MOLOCH is provided. Although the BOLAM and MOLOCH models differ in their dynamical cores, including also different choices for their vertical coordinate sets, the parameterization of atmospheric radiation, atmospheric boundary and surface layers, soil processes, and microphysical processes are common in the two models.

MOLOCH is a non-hydrostatic, fully compressible, convection-permitting model (Malguzzi et al. 2006; Davolio et al. 2009) without parameterization of convection. It employs a hybrid terrain-following vertical coordinate, depending on air density and

relaxing smoothly to horizontal surfaces away from the Earth surface. Time integration is based on an implicit scheme for the vertical propagation of sound waves, while explicit, time-split schemes are implemented for the integration of the remaining terms of the equations of motion. Three-dimensional advection is computed using the Eulerian weighted average flux scheme (Billet and Toro 1997). The atmospheric radiation is computed with a combined application of the Ritter and Geleyn (1992) scheme and the ECMWF scheme, employing 14 channels for the infrared and the visible bands (Morcrette et al. 2008). The turbulence scheme is based on an E-l, order 1.5 closure theory, where the turbulent kinetic energy equation (including advection) is evaluated (Zampieri et al. 2005). The soil model uses seven layers whose depths increase going downward, and it computes surface energy, momentum, water and snow balances, heat and water vertical transfer, vegetation effects at the surface and in the soil. It takes into account the observed geographical distribution of different soil types and soil physical parameters. The microphysical scheme, recently upgraded, was initially based on the parameterization proposed by Drofa and Malguzzi (2004). The presently applied scheme describes the conversion and interaction of cloud water, cloud ice and hydrometeors (rain, snow, graupel).

In the experiments presented below, the model chain is initialized either with NOAA-GFS or ECMWF-IFS global analyses valid at 0000 UTC of the same day of each event, 25 October and 04 November 2011, respectively. Boundary conditions are provided by the global model forecasts, available at 3-hour intervals. BOLAM integration domain covers most of Europe and the whole Mediterranean basin, using a rotated grid composed of 418x290 points at 0.1 degree spacing (about 11 km), with 50 vertical levels.

The MOLOCH experiments were all performed over an identical domain (about 780x780 km wide) with 50 atmospheric levels, at different horizontal resolutions, namely 3, 2, 1.5, and 1 km. MOLOCH is nested in the BOLAM very-short-range forecasts, starting at 0300 (0100) UTC for the CT (GE) case. This has been done in order to dynamically smooth out the sudden increase in resolution from the global data analysis to the MOLOCH grid. The orographic height used in the simulations is obtained from the NOAA dataset at 1/120° resolution (information online at www.ngdc.noaa.gov/mgg/topo/globe.html). Orography for the model grid points is obtained by interpolation and smoothing of the data.

b. The Hydro-Meteorological Forecasting Chain

The employed Hydro-meteorological Forecasting Chain (HFC) is described in Siccardi et al. (2005), Silvestro et al. (2011), and Silvestro et al. (2012), where the precipitation forecasts for the Liguria Region were provided by a number of NWP models and interpreted by expert meteorologists as explained below.

In the operational practice, Liguria is divided into five alert sub-regions (Silvestro et al. 2012), which are homogeneous from a hydro-meteorological point of view (Fig. 1). They are divided into two groups. The first group, south of the Apennines divide, has three sub-regions with basins that have their outlets in the Tyrrhenian Sea. The other group has two sub-regions that include head basins of the greater catchments that form the Po River, draining to the Adriatic Sea. The experts of HMFC of Liguria Region merge the output of the different meteorological models (the “poor man’s ensemble”) with their own experience and provide QPF for the alert sub-regions for predefined

windows of time. For each alert sub-region, a different QPF is issued. This kind of forecast is locally called a “subjective forecast”.

However, here, the QPF provided by different hindcast simulations of the MOLOCH model, implemented at different horizontal resolutions and in a real-time like configuration, is used as meteorological input. The other components of the hydro-meteorological chain are the downscaling module RainFARM and the hydrological model DRiFt (Discharge River Forecast).

DRiFt is a linear, event-scale, semi-distributed model based on a geomorphologic approach (Giannoni et al. 2000, 2005). The model focuses on the efficient description of a drainage system in its essential parts: hill-slopes and channel networks. These are addressed by using two kinematic scales that determine the base-level geomorphological response of the basin. The adopted infiltration scheme (Gabellani et al. 2008) allows the modeling of “multi-peak” events by simulating quite long periods (5–8 days) during which individual events can occur. The propagation of water in the first soil layer is described and a self-initialization of the model is produced between successive events. The schematization is applicable when the simulation period is not too long and evapotranspiration does not become crucial in the mass balance equation. The basin is discretized into cells on the basis of a Digital Elevation Model, with two velocities defining the corrivation time for each cell. The runoff estimated at cell scale is routed to the outlet section without accounting for channel storage and re-infiltration. Initial soil moisture is estimated using an Antecedent Precipitation Index (API) methodology based on the precipitation that occurred during the month preceding the event. The model has 5 parameters that are generally calibrated with the aim of reproducing the time-to-peak and

peak of streamflow values, as well as other available information regarding the stream network.

RainFARM (Rebora et al. 2006) is a downscaling model that produces an ensemble of high-resolution precipitation fields by preserving the information at the large scale derived from a QPF. The model parameters (α: spatial spectral slope; β: temporal spectral slope) are estimated on the basis of the spatial and temporal structure of the rainfall field derived by a NWP model. Once having defined l_{met} and t_{met}, the reliable spatial and temporal scales of the NWP model, RainFARM generates an ensemble (size *N*) of small-scale (e.g. spatial resolution 1 km, temporal resolution 0.5 hours) precipitation fields that are consistent with radar observations of mid-latitude precipitation events, and that maintain the volume and the spatial-temporal structure of the original rainfall field at the scale l_{met} and t_{met}. This application used N=50 ensemble members. Each precipitation field was then used as input of the hydrological model, in order to generate fifty streamflow scenarios on each catchment on the scale of one square kilometer. The results were then post-processed to produce flood forecasts. As in Silvestro et al. (2011), two different approaches to the hydrological prediction were considered: single-site and multi-catchment (Siccardi et al. 2005).

Letting l_{hydro}, t_{hydro} denote the scales of the hydrological processes (Rebora et al. 2006) and following Siccardi et al. (2005) the single-site approach was applied when $O(l_{met}/l_{hydro}) < 10^2$, while multi-catchment approach was applied when $O(l_{met}/l_{hydro}) > 10^2$. In the present application we considered as reliable meteorological scales l_{met}~15 km and t_{met}=6 hours, which are those used in the operational forecasting chain, implying that single-site approach can be applied to basins larger than 200–300 km^2. Since l_{met} is

maintained as constant, RainFARM aggregates a different number of MOLOCH rainfall pixels for different horizontal resolutions. In the case of the single-site approach, the probability that a certain flow threshold (or the flow with given return period T) is exceeded is directly evaluated.

In Liguria, a frequency analysis of the peak discharges based on a regional approach is available (Boni 2000; Boni et al. 2007). This kind of approach allows an estimation of peak flows for fixed return periods and for each basin based on two components: an index flow function of basin characteristics (i.e. drainage area) and a regional growth curve.

For smaller basins, a multi-catchment approach needs to be considered. The drawback of this method is that the forecasting procedure does not allow for any discrimination between different spatial localizations. Therefore, every basin cannot be analyzed as an independent entity, but all the basins are considered together inside domains of size l_{met} or larger.

For applications to the Liguria Region operational forecasting chain, the reference domain is assumed to be the alert sub-region. The average size of the catchments included within the alert sub-regions is on the order of 10 to 100 km^2 to the south and slightly larger to the north of the Apennine divide. For each alert sub-region a different forecast is produced. The procedure evaluates the probability that, in at least one basin of the specific alert sub-region, the flow with given return period T will be exceeded: $Pm(T) = Ie/N$, where Ie is the number of ensemble members producing a flow with return period greater than T in at least one basin. This procedure does not specify which basin will be affected due to the uncertainty associated with the meteorological forecast. The multi-

catchment procedure represents an essential paradigm in flood forecasts in very small basins (Siccardi et al. 2005) for those involved in civil protection at both the scientific and political levels of decision making.

3. Meteorological perspective

a. The Case studies

A detailed description and a hydro-meteorological characterization of both events can be found in Rebora et al. (2013) and Buzzi et al. (2014), while more details on the GE case are reported in Silvestro et al. (2012) and Fiori et al. (2014). However, for the sake of clarity, the main synoptic and mesoscale aspects are described below.

Both heavy precipitation events were associated with a deep low-pressure system located close to the British Isles and a large scale Atlantic trough that progressively deepened over the Mediterranean basin, and were characterized by an upper-level positive potential vorticity (PV) anomaly over Western Europe. This pattern also produced an intense moist air advection from subtropical areas and induced a upper-level diffluent southwesterly flow over the Liguria Region, supporting upward motion. In the GE case, moreover, the moisture content was significantly enhanced by the remnants of the tropical storm Rina (Silvestro et al. 2012), which had merged with the mid-latitude storm track few days earlier. Due to the presence of a pressure ridge over Eastern Europe, the eastward progression of the synoptic wave and of the associated frontal system was slow, keeping the precipitation systems largely stationary. A moist low-level southeasterly jet over the Tyrrhenian Sea developed, channeled between Corsica and the Italian coast. At the same time, the cold air mass formed in the previous days over the Po

Valley was forced to flow southward across the gaps in the Apennines, reaching the Ligurian Sea in response to intense low-level winds entering the Po Valley from the Adriatic side. This complex wind pattern produced a sharp convergence line over the Ligurian Sea (Fig. 12 of Buzzi et al. (2014) clearly illustrates the described convergence pattern), as observed and confirmed by satellite data analysis, where the convective activity was triggered and then sustained by the presence of convective available potential energy (CAPE) and remarkable vertical wind shear. Wind direction turned from southeasterly to southwesterly within 2000 meters from the surface.

In the CT event, the convective activity organized in association with a similar convergence line, where different convective cells developed and regenerated during the day. As revealed by radar observations, these cells formed along a convective line over the sea and moved towards an area where complex orography played a role in focusing and amplifying the precipitating cells. The accumulated rainfall (Fig. 2) was exceptional both in terms of the hourly rain rate (with a peak of 150 mm/h) and of the total precipitation (more than 500 mm in 12 hours).

The GE case was characterized by a pre-frontal mesoscale convective system (MCS) that formed in association with a convergence line, which remained almost stationary near the city of Genoa until the synoptic front swept over the region, steering the MCS with it. Again, localized and exceptional precipitation affected the region. Rain-gauge measurements exceeded 180 mm/h and registered more than 500 mm totally (Fig. 3).

Buzzi et al. (2014) identified some further mesoscale aspects responsible for differences in the development of the two systems and, consequently, for differences in

their rainfall. It is relevant for this study to highlight the differences between the thermodynamic profiles characterizing the air masses within the low-level jet over the Tyrrhenian Sea, feeding the convective systems (Fig. 4). MOLOCH simulations reveal that, although CAPE values are similar (of the order of 1000 J kg^{-1}), the CT event is characterized by a larger instability, the level of free convection (LFC) being very close to the surface. Conversely, the thermodynamic diagram for the GE case clearly shows that a relevant vertical forcing is needed in order to overcome the inhibition, the LFC being pretty high (around 1500 m). The orographic uplift over the Apennine may have contributed, to some extent, providing the forcing that triggered the convection. These characteristics appear realistic when compared with observations: during the CT event, rainfall was widespread over the Ligurian Sea; while in the GE case, rainfall was more concentrated and close to the coast.

b. Numerical Results

For the CT case, the most satisfactory MOLOCH QPF is obtained by initializing the NWP chain with NOAA-GFS global analysis. Although the differences are not remarkable, GFS-based MOLOCH simulations provide more intense rainfall maxima than IFS-based runs. Figure 5 shows the total accumulated precipitation forecast by MOLOCH at different horizontal grid spacings. Heavy precipitation is located over the coastal orographic range and the Apennines near the border between Liguria and Tuscany. The rainfall intensity over the area affected by the flood tends to increase going from 3 km to 1.5 km grid spacing, with maximum values accumulated in 18 hours rising from 175 mm to 318 mm, respectively, thus getting closer to the observed exceptional

amount of about 500 mm. Moving to the highest horizontal resolution simulation (1 km), the rainfall maximum presents a slightly lower absolute value, about 300 mm. However, it is worth noting that, in the 1 km mesh size run, the spatially integrated precipitation is somewhat larger (integrated precipitation generally increases with increasing model resolution). By analyzing the hourly evolution of the rainfall field (not shown) at the highest resolution, it becomes clear that the model produces more scattered convective cells affecting slightly different inland areas. The final picture is thus characterized by a less compact structure of the rainfall field.

For the GE event, better results are obtained using ECMWF-IFS analysis. MOLOCH forecast precipitation is shown in Fig. 6. As described earlier, the rainfall is concentrated near the MCS rather than being widespread over the sea, which agrees with available radar observations. In this case, rainfall maxima increase steadily with increasing model horizontal resolution, from 199 mm to 352 mm in 18 hours. The evolution of the MCS is qualitatively similar in the four forecasts, but its intensity remarkably improves at high-resolution. Moreover, as the grid spacing decreases, the MCS is shifted progressively eastward, getting closer to the observed position where most of the heavy rainfall was recorded. As expected, the high-resolution allows for a more accurate representation of the small-scale mechanisms involved in the MCS dynamics, including its interaction with the orography, and for the accurate simulation of the low-level convergence line, which is a crucial factor for the correct prediction of the MCS position. MOLOCH simulations are able to correctly reproduce the “finger-like” structure (Parodi et al. 2012) observed from remote sensing platforms only at suitably high horizontal resolution (less than 2 km).

4. Impacts on Flood Forecast

Hydrological verification was done using the simulations obtained by feeding DRiFt with the observed rainfall as benchmark. Observed streamflow is available only for a small number of modeled sections. However, different analyses of the event show that the hydrological simulations accurately reproduced what effectively happened in terms of peak flows (see, for example, Silvestro et al. 2012). Since the objective is to evaluate the impact of different NWP chain configurations (i.e. initialization and MOLOCH horizontal resolution), an analysis of the hydrological model performance with respect to streamflow observations is out of the scope of this work. The modeled hydrograph (Berenguer et al. 2005) is thus assumed as truth (or reference). The time range of the meteorological forecasts is 24 hours. The length of the hydrological simulation is equal to the time range of the meteorological forecasts plus twice the concentration time of the basin, which is assumed to be 12 hours.

a. CT Event: 25 October 2011

The CT event mainly hit the alert sub-region C (Figs. 1 and 2), in the eastern part of the Liguria Region. The most relevant effects in terms of streamflow occurred on the Vara and Magra basins. Vara is a tributary of the Magra River with an area of about 600 km^2. The entire Magra basin, closed at its outlet in the Mediterranean Sea, has an area of 1660 km^2. Several very small basins along the western coast of Liguria (the Cinque Terre region) were affected by the flood. However, they are not operationally modeled by the HFC operational at the HMFC.

In Fig. 7, the results of the multi-catchment approach are reported. The panels show the impact on flood prediction of different MOLOCH horizontal resolutions and of different global analyses used to initialize the NWP chain. On the X axis the return period T is shown, while the Y axis reports the probability that at least one basin that belongs to alert sub-region C will exceed a certain T. As a reference point, the maximum T (hereafter observed T) that occurred during the event in a modeled section belonging to the sub-region C is shown by the red vertical line. All the HFC configurations underestimate the flood intensity, since the occurrence of observed T always has a negligible or null probability. In terms of real-time decisions, whether such a prediction could have brought forecasters to issue an alert would strongly depend on the experience of the forecasters themselves. A posteriori evaluation of the probabilistic forecasts may be done using ad-hoc techniques (Panziera et al. 2013), but from an operational point of view this matter is quite tricky, since the benchmark of the observed T is not available during real-time operations. However, the interesting and encouraging result is that the performance of the chain improves with increasing MOLOCH resolution, at least up to a certain point. This is more evident with the chain initialized with GFS. This improvement can be clearly noted until the 1.5 km grid mesh size; a further decrease in grid spacing (from 1.5 to 1 km) does not correspond to a significant improvement in the multi-basin discharge prediction. The latter result is consistent with the meteorological discussion of Section 3b.

The single-site results are presented for three significant sections of the Magra basin: the two sections upstream where the Vara and Magra join, and the outlet to the sea. The results are presented in terms of box plot of the peak flows for every basin (Fig. 8). A

box plot is built for each of the three selected sections; on the X axis the drainage area is reported, while on the Y axis the peak flows normalized with the index flow (Boni 2000; Boni et al. 2007) are shown. The normalized peak flows obtained using observed precipitation as input into the hydrological chain are indicated (diamonds) and represent the benchmark. The underestimation of the discharges is again evident: the benchmarks are always outside and at higher values than both the boxes representing the interquartile and the whiskers corresponding to the maximum range. This means that all the streamflow scenarios are always lower than the benchmark. Again the trend is good since the values associated with boxes and whiskers increase somewhat, getting closer to the benchmark, for the discharges driven by the 1.5 km (1 km) MOLOCH prediction driven by the ECMWF (GFS) global model.

b. GE Event: 04 November 2011

In the GE case, floods mainly hit the alert sub-region B (Figs. 1 and 3), in the central part of the Liguria Region. The event was really concentrated in and affected with particular severity a portion of the city of Genoa, causing the flooding of the Bisagno creek and of its tributary the Fereggiano. As for the CT event, the discharge forecasts (Fig. 9) underestimated the severity of the episode, but the improvements achieved by increasing MOLOCH spatial resolution are evident for both NWP modeling chains, either initialized with GFS or ECMWF data. The 3 km resolution configuration hardly caught the event in terms of hydrological response, since the rainfall maximum (Fig. 6a) was greatly underestimated and located to the west of the observed position. However, feeding the hydrological chain with the 1-km-resolution MOLOCH rainfall field yielded

T=5 years with probability 30% (60%) and T=10 years with probability 5% (10%) for GFS (ECMWF) initialization. Again, the hydrological prediction confirmed the meteorological analysis of the previous section. In the GE case, very high-resolution is required in order to properly represent the small-scale features associated with the isolated MCS, both during the triggering phase and the mature stage, in order to represent the important role played by the orography. The increase of rainfall intensity and the eastward displacement of the precipitation maximum with increasing MOLOCH horizontal resolution produced a better agreement with rain-gauge observations and, consequently, an improvement of the discharge forecasts.

Results of the single-site approach are not presented because all the basins belonging to sub-region B have a drainage area smaller than 200 km^2.

5. Discussion and Conclusions

This paper showed the implications for flood forecasting of improving the horizontal resolution of the NWP system used as input of an operational probabilistic hydrological forecasting chain for two severe flood events in the Liguria Region (Northern Italy). Moreover, the impact of two possible initializations of the NWP system, using NCEP-GFS or ECMWF-IFS global model data, was investigated. The whole model chain – composed of two meteorological models applied in succession to attain high-resolution QPF (BOLAM-MOLOCH), a rainfall downscaling module (RainFARM), and a hydrological model (DRiFt) – was implemented for two major floods that occurred during autumn 2011. In this way, QPF provided by different configurations of the

meteorological modeling chain was validated in a pragmatic framework through an operational flood forecasting system.

Results were different in the two cases, mainly because the two events presented different meteorological characteristics (Buzzi et al. 2014) during both the convection-triggering phase and the subsequent development of the most intense rainfall. In the GE event (04 November 2011), higher spatial resolution resulted more clearly in an improved QPF, due to a better description of the isolated MCS and of its interaction with the orography. The positive impact due to the reduction of the horizontal grid spacing was confirmed also in terms of hydrological predictions, since the flood forecasting results were remarkably improved. High NWP resolution also turned out to be beneficial for discharge prediction for the CT event (25 October 2011), although to a lesser extent. The meteorological evolution in this case was characterized by a more unstable low-level flow that produced less organized convection; the precipitating systems were less connected to the mesoscale convergence line over the sea that provided an extended range of predictability with respect to scattered convective activity (Buzzi et al. 2014). However, even considering the best setup in terms of driving global model and MOLOCH horizontal resolution, the severity of the floods was underestimated, at least in terms of peak-flows, in both events.

Although the multi-catchment approach was not able to provide information about the exact location of the forecast maximum discharge, it was particularly suitable for model validation since it took into account possible and unavoidable uncertainties in the QPF. In fact, displacement errors that occur quite often with convective systems that develop over complex orography can be relevant for hydrological applications, especially

when dealing with single, small-size catchments such as those characterizing the Liguria territory. In this case, the uncertainties related to the different scales of the meteorological forecasts and the hydrological response are emphasized by the unpredictability of the correct localization and intensity of the most intense rainfall structures. The multi-catchment method tries to deal with the difficulty of discriminating between one basin and another, expressing the forecast in terms of the probability of exceeding a flow within a given return period on pre-defined regions. It highlights possible critical situations even when their probability is very low (when considering the forecast for each single basin separately).

Employing higher-resolution configurations surely would have helped predict in both the cases here analyzed, that events of considerable intensity were going to occur and allowed warnings to be issued. This is especially evident for the GE event: the lowest horizontal resolution run generated a discharge prediction typical of a normal rainfall event while the high-resolution forecasts indeed produced severe rainfall and discharge scenarios that would have led to the issuing of a warning or an alert. A civil protection system usually defines only a limited number of alert levels, and in the case of Liguria Region only two alert levels can be issued (Silvestro et. al 2012), based on the subjective decision of the forecaster and on how much risk the decision maker is willing to take. Since issuing alerts is a threshold process, once the forecaster or the decision maker has decided to issue the maximum level of alert, nothing more can be done from the point of view of the forecast, and it does not actually matter if the event turns out to be more severe than expected. In fact, at that point the civil protection machine has been primed and the authorities in charge of performing actions (e.g. regional and municipal figures

police, firefighters) must carry out the measures needed to reduce damages and casualties. We cannot state with certainty what level of alert would have been issued if the high-resolution chains here described had been available at the time of the events (Ramos et al. 2013, provides a clear insight on the critical role of decision makers in flood forecasting), but we are confident in stating that the 1–1.5 km horizontal resolution configurations produced flood forecasts severe enough to alert decision makers to the potential for a dangerous event.

These results cannot be considered as general, since two case studies are certainly not enough to draw robust conclusions. However, since the meteo-hydrological chain has been already set up, it will be possible to verify the present results for other events, in particular those that occurred during the HyMeX SOP1 field campaign, exploiting the availability of detailed observations.

Finally, it must be noted that a very recent event, the Genoa flood of 9 October 2014, with characteristics very similar to those described above, caused one casualty and damages estimated at hundred of millions of euros. Most of the models initialized the morning of 9 October severely under-predicted the total precipitation. Again, preliminary experiments performed on this new flood episode emphasize the crucial role that employing high-horizontal resolution meteorological models could play, and how important is to provide these tools to forecasters and decision makers as quickly as possible.

Acknowledgments.

This work represents a contribution to the HyMeX international program. This work was supported by the Civil Protection of Italy under contract "Intesa Operativa con CNR-ISAC" and by the Italian flagship project RITMARE. We thank Gregory J. Carbone and Karen Beidel for kindly reviewing the manuscript. We also thank three anonymous reviewers for their comments, which helped improve this manuscript.

References

Berenguer, M., C. Corral, R. Sanchez-Diesma, and D. Sempere-Torres, 2005: Hydrological validation of a radar-based nowcasting technique, *J. Hydrometeor*., **6**, 532-549.

Billet, S., and E. F. Toro, 1997: On WAF-type schemes for multidimensional hyperbolic conservation laws. *J. Comput. Phys*., **130**, 1–24.

Boni, G., 2000: A physically based regional rainfall frequency analysis: application to a coastal region in Northern Italy. *Proc. EGS Plinius Conf. on Mediterranean Storms, Italy*, 365-376.

Boni, G., L. Ferraris, F. Giannoni, G. Roth, and R. Rudari, 2007: Flood probability analysis for un-gauged watersheds by means of a simple distributed hydrologic model. *Adv. Water Resour.*, **30(10)**, 2135-2144, doi:10.1016/j.advwatres.2006.08.009.

Buzzi, A., M. D'Isidoro, and S. Davolio, 2003: A case study of an orographic cyclone south of the Alps during the MAP SOP. *Q. J. R. Meteorol. Soc*. **129**, 1795-1818.

Buzzi, A., S. Davolio, P. Malguzzi, O. Drofa, and D. Mastrangelo, 2014: Heavy rainfall episodes over Liguria of autumn 2011: numerical forecasting experiments. *Nat. Hazards Earth Syst. Sci*., **14**,1325-1340.

Cloke, H. L., and F. Pappenberger, 2009: Ensemble Flood Forecasting: a review. *J. Hydrol.*, **375(3-4)**, 613-626.

Cuo, L., T. C. Pagano, and Q. J. Wang, 2011: A review of quantitative precipitation forecasts and their use in short- to medium-range streamflow forecasting. *J. Hydrometeor*., **12**, 713-728.

Davolio, S., and A. Buzzi, 2004: A nudging scheme for the assimilation of precipitation data into a mesoscale model. *Wea. Forecasting,* **19**, 855–871.

Davolio, S., A. Buzzi, and P. Malguzzi, 2009: Orographic triggering of long-lived convection in three dimensions. *Meteor. Atmos. Phys*., **103**, 35-44.

Drobinski, P., V. Ducrocq, P. Alpert, E. Anagnostou, K. Béranger, M. Borga, I. Braud, A. Chanzy, S. Davolio, G. Delrieu, C. Estournel, N. Filali Boubrahmi, J. Font, V. Grubisic, S. Gualdi, V. Homar, B. Ivancan-Picek, C. Kottmeier, V. Kotroni, K. Lagouvardos, P. Lionello, M. C. Llasat, W. Ludwig, C. Lutoff, A. Mariotti, E. Richard, R. Romero, R. Rotunno, O. Roussot, I. Ruin, S. Somot, I. Taupier-Letage, J. Tintore, R. Uijlenhoet, and H. Wernli, 2013: HyMeX, a 10-year multidisciplinary program on the Mediterranean water cycle. *Bull. Amer. Meteor. Soc*., **95**, 1063-1082, doi: 10.1175/BAMS-D-12-00242.1.

Drofa, O., and P. Malguzzi, 2004: Parameterization of microphysical processes in a non hydrostatic prediction model. *Proc. 14th Intern. Conf. on Clouds and Precipitation, Italy,* 1297-3000.

Ducrocq, V., I. Braud, S. Davolio, R. Ferretti, C. Flamant, A. Jansa, N. Kalthoff, E. Richard, I. Taupier-Letage, P.-A. Ayral, S. Belamari, A. Berne, M. Borga, B. Boudevillain, O. Bock, J.-L. Boichard, M.-N. Bouin, O. Bousquet, C. Bouvier, J. Chiggiato, D. Cimini, U. Corsmeier, L. Coppola, P. Cocquerez, E. Defer, P. Drobinski, Y. Dufournet, N. Fourrié, J. J. Gourley, L. Labatut, D. Lambert, J. Le Coz, F. S. Marzano, G. Molinié, A. Montani, G. Nord, M. Nuret, K. Ramage, B. Rison, O. Roussot, F. Said, A. Schwarzenboeck, P. Testor, J. Van Baelen, B. Vincendon, M. Aran, and J. Tamayo, 2013: HyMeX-SOP1, the field campaign dedicated to heavy precipitation and flash flooding in the northwestern Mediterranean. *Bull. Amer. Meteor. Soc*., **95**, 1083-1100 doi: 10.1175/BAMS-D-12-00244.1.

Ferretti, R., E. Pichelli, S. Gentile, I. Maiello, D. Cimini, S. Davolio, M. M. Miglietta, G. Panegrossi, L. Baldini, F. Pasi, F. S. Marzano, A. Zinzi, S. Mariani, M. Casaioli, G. Bartolini, N. Loglisci, A. Montani, C. Marsigli, A. Manzato, A. Pucillo, M. E. Ferrario, V. Colaiuda, and R. Rotunno, 2014.: Overview of the first HyMeX Special Observation Period over Italy: observations and model results. *Hydrol. Earth Syst. Sc*., **18**,1953-1977.

Fiori, E., A. Comellas, L. Molini, N. Rebora, F. Siccardi, D. J. Gochis, S. Tanelli, and A. Parodi, 2014: Analysis and hindcast simulations of an extreme rainfall event in the Mediterranean area: The Genoa 2011 case. *Atmos. Res.*, **138**, 13-29.

Fundel, F., A. Walser, M. A. Liniger, C. Frei, and C. Appenzeller, 2010: Calibrated precipitation forecasts for a limited-area ensemble forecast system using reforecasts, *Mon. Wea. Rev*, **138**, 176 – 189.

Gabellani, S., F. Silvestro, R. Rudari, and G. Boni, 2008: General calibration methodology for a combined Horton-SCS infiltration scheme in flash flood modeling, *Nat. Hazards Earth Syst. Sci*., **8**, 1317 - 1327.

Gerogakakos, K., and E. Foufola Georgiou, 1991: Real time coupling of hydrologic and meteorological models for flood forecasting, *Recent Advances in the modeling of Hydrologic systems, NATO ASI Series*, **354**, 169-184.

Ghile, Y. B., and R. E. Schulze, 2010: Evaluation of three numerical weather prediction models for short and medium range agrohydrological applications. *Water Res. Manag.*, **24**, 1005-10028.

Giannoni, F., G. Roth, and R. Rudari, 2005: A procedure for drainage network identification from geomorphology and its application to the prediction of the hydrologic response. *Adv. Water Resour.*, **28(6)**, 567-581, doi:10.1016/j.advwatres.2004.11.013.

Hohenegger, C., and C. Schär, 2007: Atmospheric predictability at synoptic versus cloud-resolving scales. *Bull. Amer. Meteor. Soc*., **88**, 1783–1793.

Kain, J.S., 2004: The Kain-Fritsch convective parameterization: an update. *J. Appl. Meteor*., **43**, 170-181.

Malguzzi, P., G. Grossi, A. Buzzi, R. Ranzi, and R. Buizza, 2006: The 1966 'century' flood in Italy: A meteorological and hydrological revisitation. *J. Geophys. Res*., **111**, D24106, doi:10.1029/2006JD007111.

Morcrette, J.-J., H. W. Barker, J. N. S. Cole, M. J. Iacono, and R. Pincus, 2008: Impact of a new radiation package, McRad, in the ECMWF Integrated Forecasting System. *Mon. Wea. Rev.*, **136**, 4773-4798.

Pappenberger, F., K. Scipal, and R. Buizza, 2008: Hydrological aspects of meteorological verification. *Atmos. Sci. Lett*., **9**, 43-52.

Parodi, A., G. Boni, L. Ferraris, F. Siccardi, P. Pagliara, E. Trovatore, E. Foufoula-Georgiou, and D. Kranzlmueller, 2012: The "perfect storm": from across the Atlantic to the hills of Genoa. *EOS*, **39**, No. 24, 225-226.

Ramos, M. H., S. J. van Andel, and F. Pappenberger, 2013: Do probabilistic forecasts lead to better decisions? *Hydrol. Earth Syst. Sci.,* **17**, 2219-2232.

Rebora, N., L. Ferraris, J. H. Hardenberg, and A. Provenzale, 2006: The RainFARM: Rainfall Downscaling by a Filtered Auto Regressive Model. *J. Hydrometeor*., **7**, 724-738.

Rebora, N., L. Molini, E. Casella, A. Comellas, E. Fiori, F. Pignone, F., Siccardi, F. Silvestro, S. Tanelli, and A. Parodi, 2013: Extreme rainfall in the Mediterranean: what can we learn from observations? *J. Hydrometeor*., **14**, 906-922.

Ritter, B., and J. F. Geleyn, 1992: A comprehensive radiation scheme for numerical weather prediction models with potential applications in climate simulations. *Mon. Wea. Rev.*, **120**, 303-325.

Roberts, N. M., S. J. Cole, R. M. Forbes, R. J. Moore, and D. Boswell, 2009: Use of high-resolution NWP rainfall and river flow forecasts for advance warning of the Carlisle flood, north-west England. *Meteor. Appl*., **16**, 23-34.

Siccardi, F., G. Boni, L. Ferraris, and R. Rudari, 2005: A hydro-meteorological approach for probabilistic flood forecast. *J. Geophys. Res*, **110**, d05101, doi:10.1029/2004jd005314.

Silvestro, F., N. Rebora, and L. Ferraris, 2011: Quantitative flood forecasting on small and medium size basins: a probabilistic approach for operational purposes. *J. Hydrometeor*., **12(6)**, 1432-1446.

Silvestro, F., S. Gabellani, F. Giannoni, A. Parodi, N. Rebora, R. Rudari, and F. Siccardi, 2012: A hydrological analysis of the 4th November 2011 event in Genoa. *Nat. Hazards Earth Syst. Sci.,* **12**, 2743-2752, doi:10.5194/nhess-12-2743-2012.

Westrick, K. J., and C. F. Mass, 2001: An evaluation of a high-resolution hydrometeorological modeling system for prediction of a cool-season flood event in a coastal mountainous watershed. *J. Hydrometeor*., **2**, 161-180.

WMO, 1992: Manual on the global data-processing and forecasting system. *WMO-No. 485*, **Vol. 1**, pp. 153, ISBN 92-63-12485-X.

Zampieri, M., P. Malguzzi, and A. Buzzi, 2005: Sensitivity of quantitative precipitation forecasts to boundary layer parameterization: a flash flood case study in the Western Mediterranean. *Nat. Hazard Earth Syst. Sci*., **5**, 603-612.

List of Figures

FIGURE 6. Precipitation accumulated in the 18-hour period starting at 0300 UTC, 04 Nov 2011 in MOLOCH forecast runs, based on ECMWF-IFS analysis at 0000 UTC of the same day, for different horizontal resolution: 3.0 km, max. 199 mm (a), 2.0 km, 249 mm (b), 1.5 km, 266 mm (c), 1.0 km, 352 mm (d).

FIGURE 7. CT event (25 Oct 2011). Results for the multi-catchment hydrological approach using the NWP chain driven by ECMWF (upper panels) and GFS (lower panels) models, for different MOLOCH horizontal resolutions. X-axis: return period T. Y-axis: probability of exceeding the return period in at least one basin within the considered region. The red vertical line indicates the maximum observed T.

FIGURE 8. CT event (25 Oct 2011). Results for the single-site approach using the NWP chain driven by ECMWF (upper panels) and GFS (lower panels), for different MOLOCH horizontal resolutions, at three significant outlet sections. X-axis: dimension of the drainage area of the three basins. Y-axis: normalized peak flow (see text). Diamonds indicate the normalized peak flows obtained using observed precipitation as input of the hydrological chain.

FIGURE 9. GE event (04 Nov 2011). Results for the multi-catchment hydrological approach using the NWP chain driven by ECMWF (upper panels) and GFS (lower panels), for different MOLOCH horizontal resolutions. X-axis: return period T. Y-axis: probability of exceeding the return period in at least one basin within the considered region. The red vertical line indicates the maximum observed T.

1

2

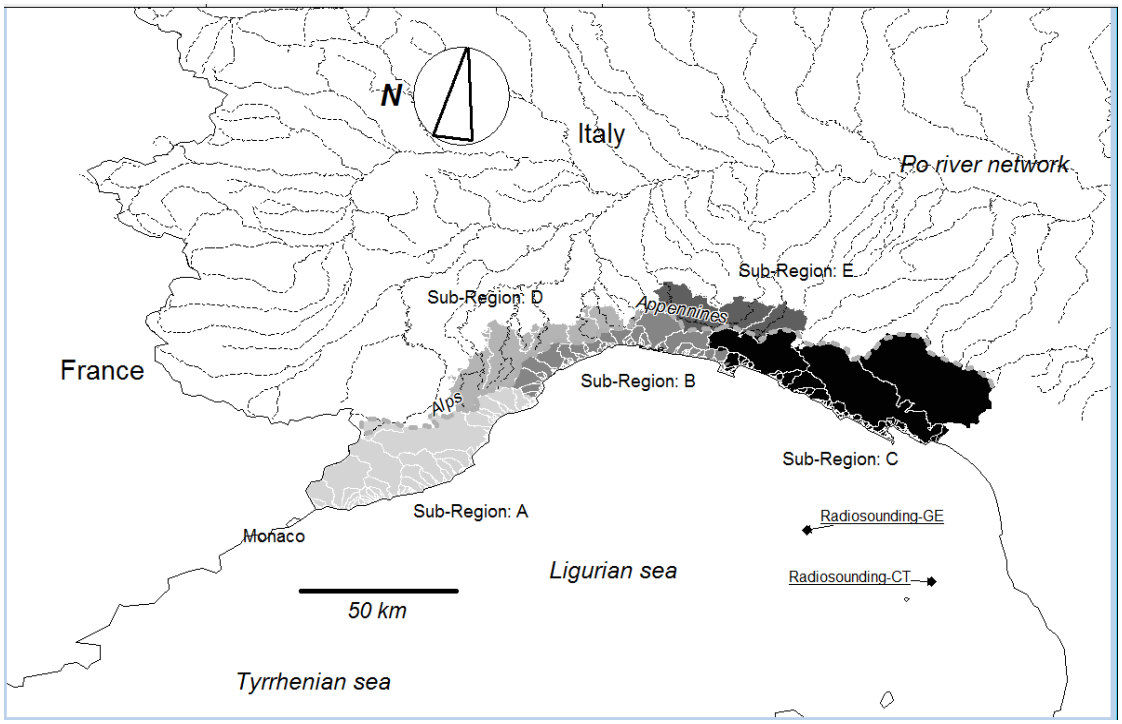

FIGURE 1. Liguria Region, Northern Italy. Homogeneous sub-regions are reported in grey tones. Locations of the simulated soundings shown in Fig. 4 are also indicated.

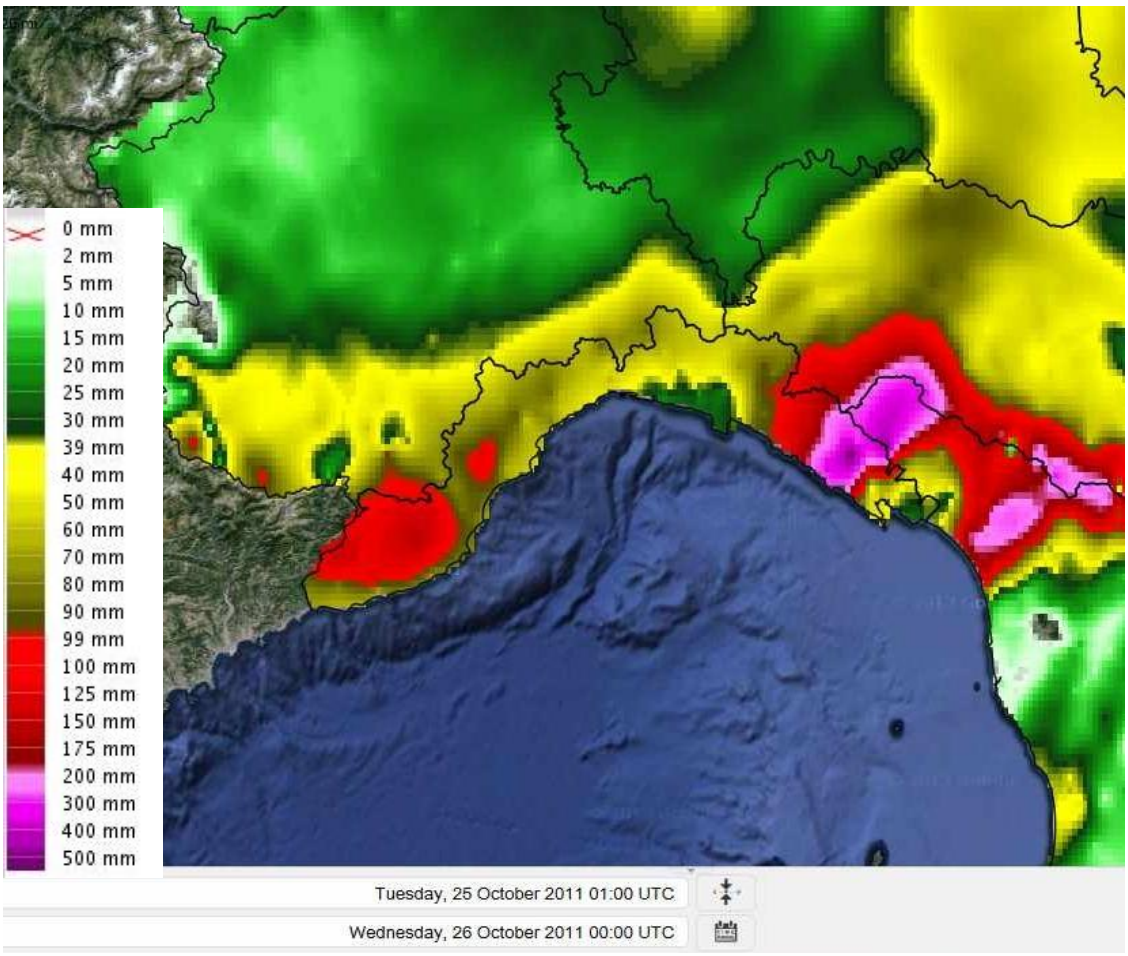

FIGURE 2. 24-hour accumulated rainfall on 25 Oct. 2011 for the CT event, estimated by the interpolation of gauge measurements.

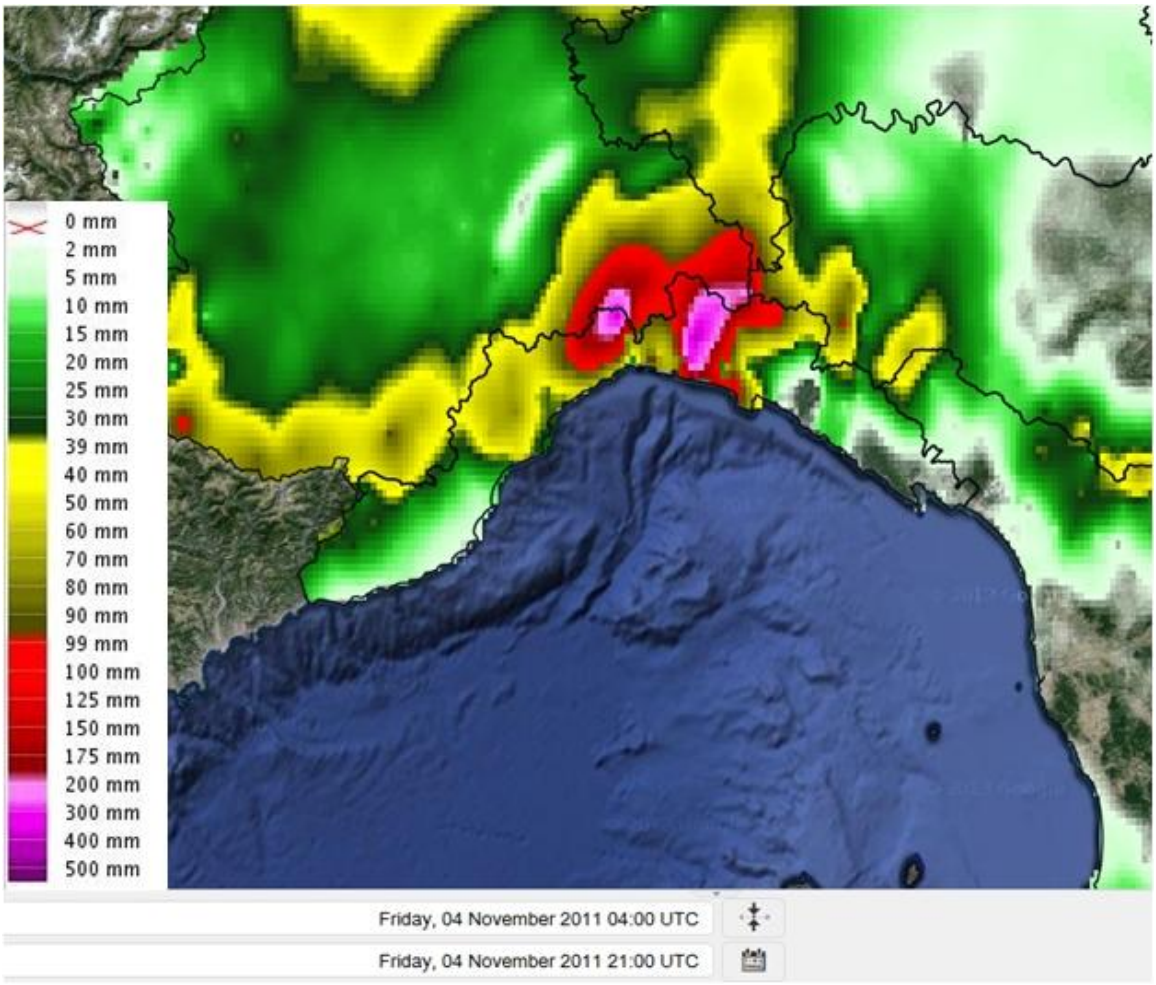

FIGURE 3. 18-hour accumulated rainfall on 04 Nov 2011 at 2100 UTC, for the GE event, estimated by the interpolation of gauge measurements.

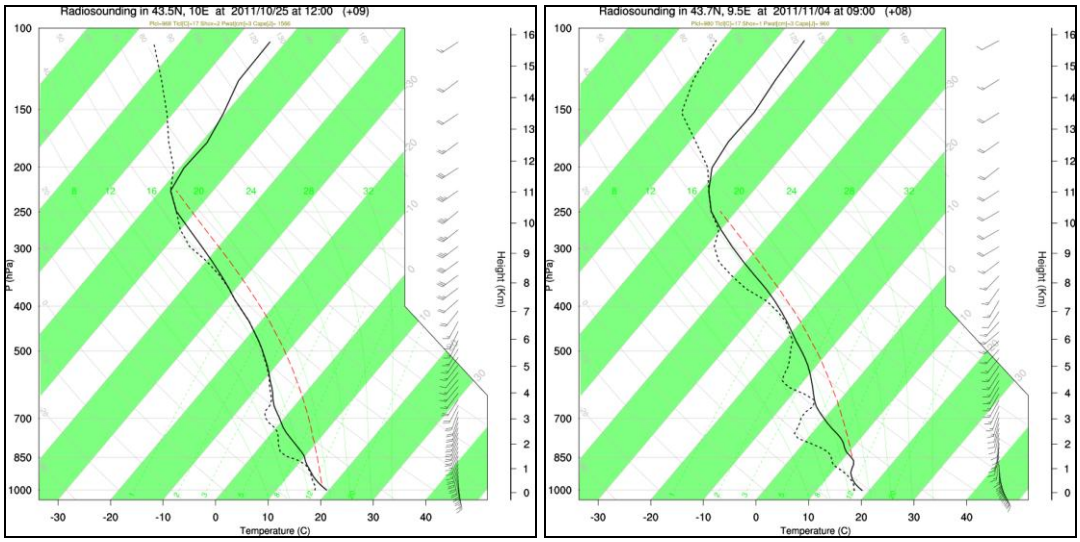

FIGURE 4. Vertical profiles simulated by the MOLOCH model at 1.5 km horizontal resolution during the early stage of precipitation, taken upstream of the precipitating system, by averaging over the grid points within a small area of about 50x50 km. Left panel: CT event, 25 Oct 2011, 1200 UTC, centered at 43.5N, 10E. Right panel: GE case, 04 Nov 2011, 0900 UTC, centered at 43.7N, 9.5E. The profile locations are shown in Fig. 1.

1

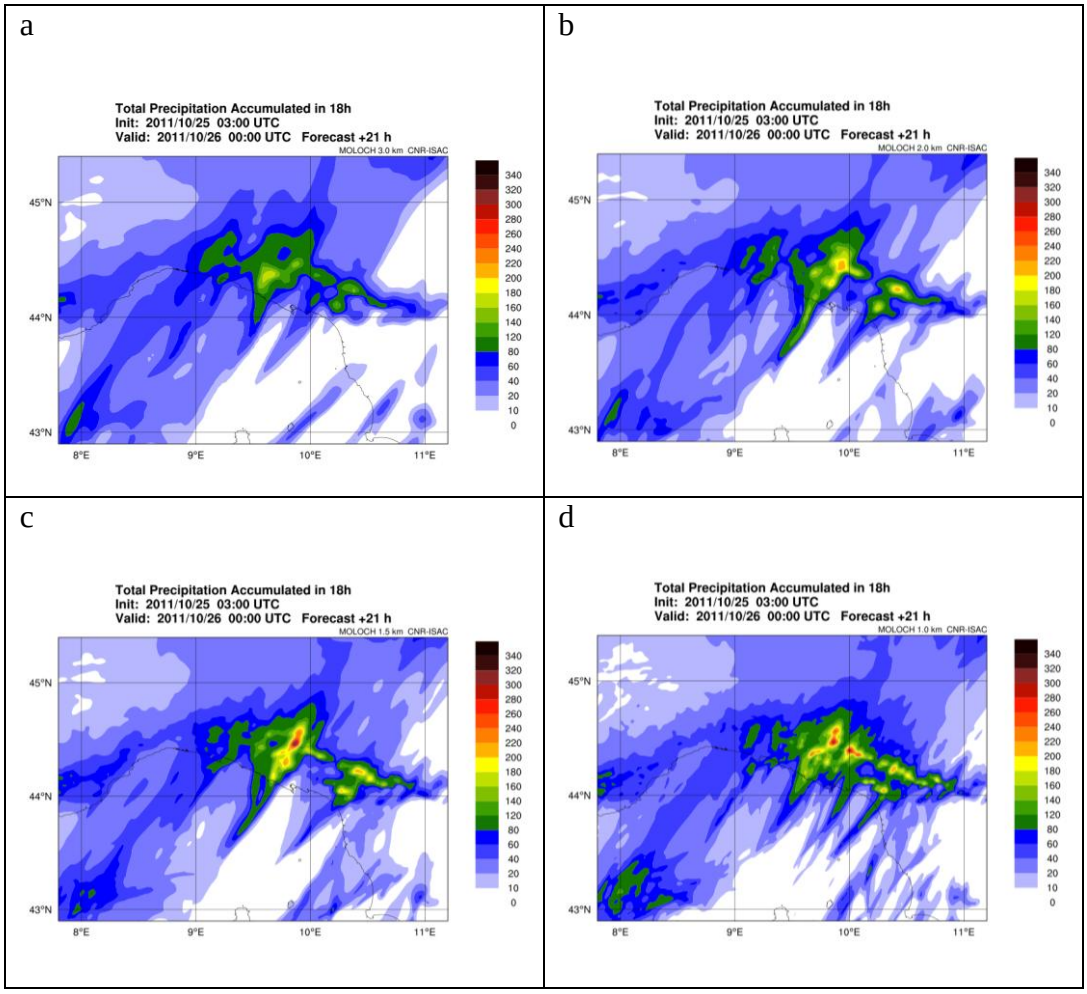

2

3 FIGURE 5. Precipitation accumulated in the 18-hour period starting at 0600 UTC, 25 Oct
4 2011 in MOLOCH forecast runs, based on NOAA-GFS analysis at 0000 UTC of the
5 same day, for different horizontal resolutions: 3.0 km, max. 175 mm (a), 2.0 km, 215 mm
6 (b), 1.5 km, 318 mm (c), 1.0 km, 299 mm (d).

7

8

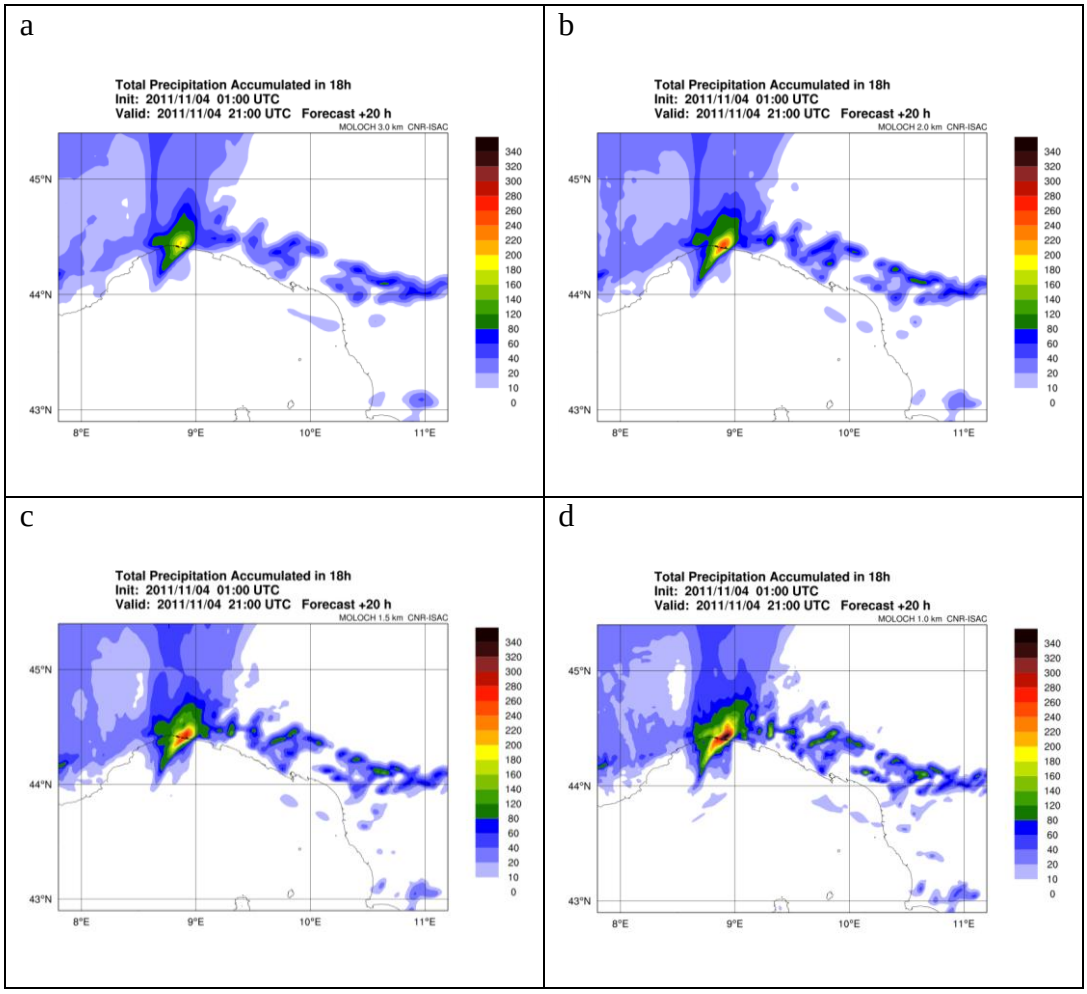

FIGURE 6. Precipitation accumulated in the 18-hour period starting at 0300 UTC, 04 Nov 2011 in MOLOCH forecast runs, based on ECMWF-IFS analysis at 0000 UTC of the same day, for different horizontal resolution: 3.0 km, max. 199 mm (a), 2.0 km, 249 mm (b), 1.5 km, 266 mm (c), 1.0 km, 352 mm (d).

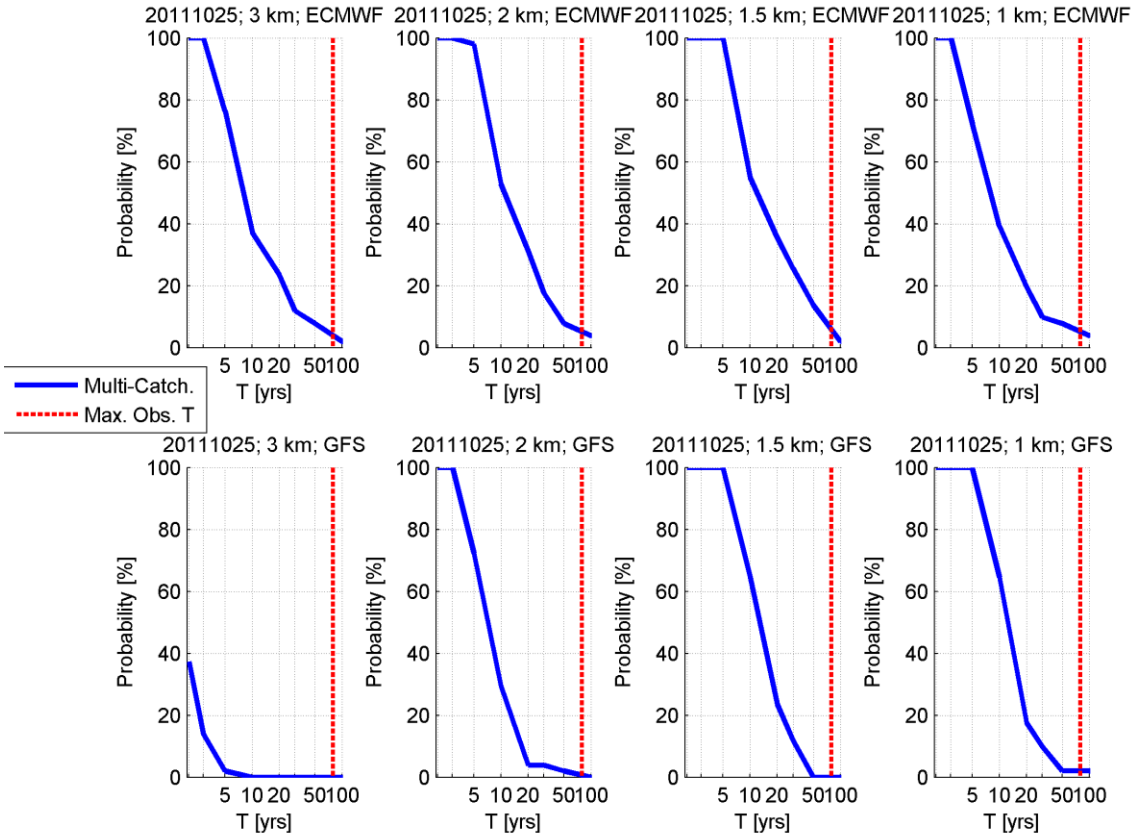

FIGURE 7. CT event (25 Oct 2011). Results for the multi-catchment hydrological approach using the NWP chain driven by ECMWF (upper panels) and GFS (lower panels) models, for different MOLOCH horizontal resolutions. X-axis: return period T. Y-axis: probability of exceeding the return period in at least one basin within the considered region. The red vertical line indicates the maximum observed T.

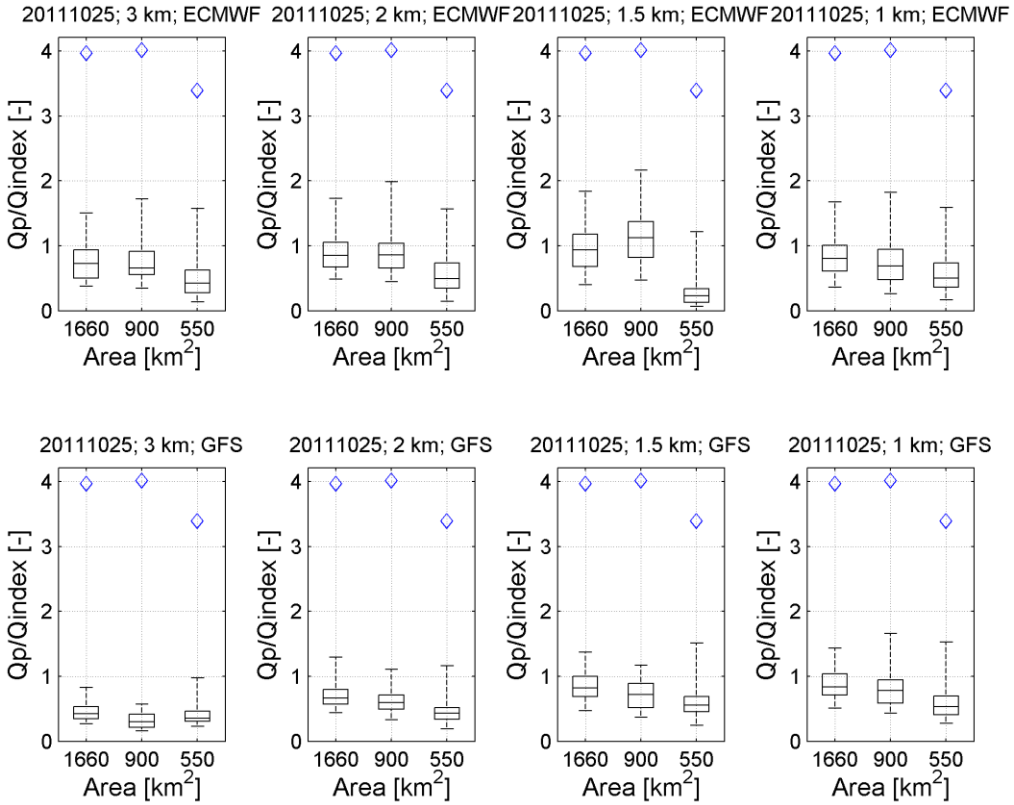

FIGURE 8. CT event (25 Oct 2011). Results for the single-site approach using the NWP chain driven by ECMWF (upper panels) and GFS (lower panels), for different MOLOCH horizontal resolutions, at three significant outlet sections. X-axis: dimension of the drainage area of the three basins. Y-axis: normalized peak flow (see text). Diamonds indicate the normalized peak flows obtained using observed precipitation as input of the hydrological chain.

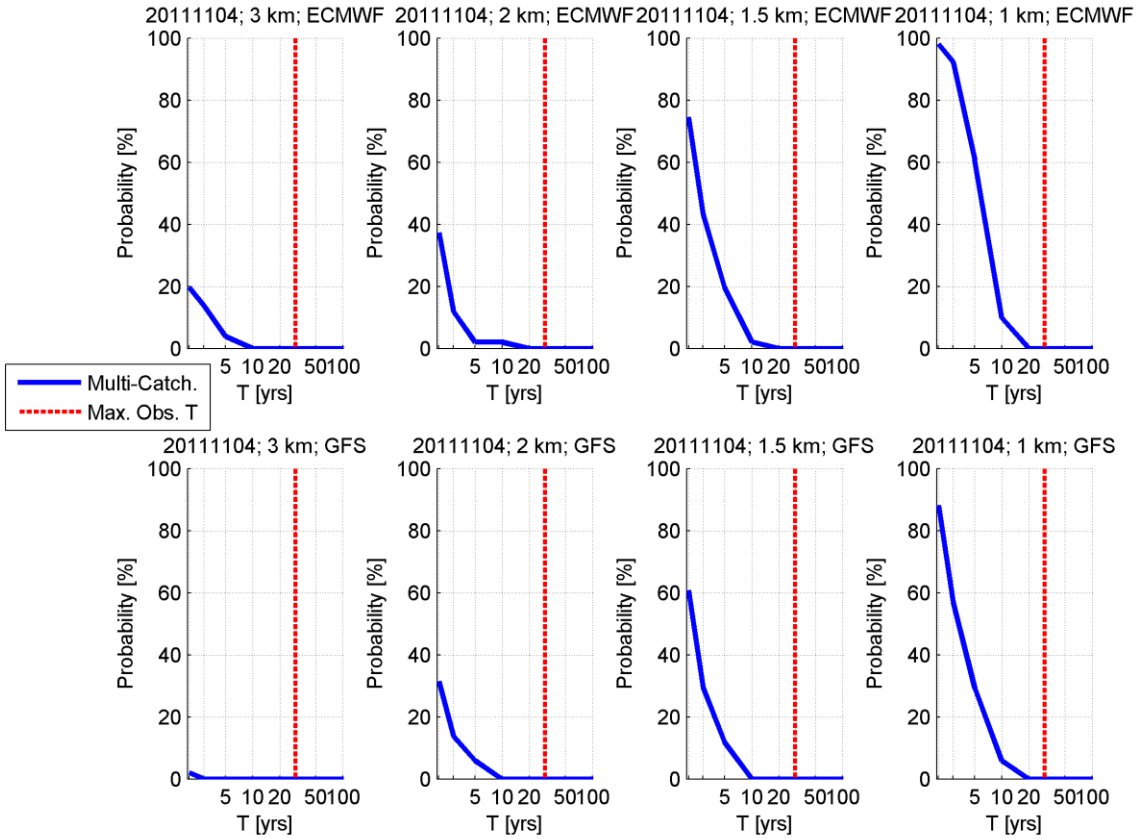

FIGURE 9. GE event (04 Nov 2011). Results for the multi-catchment hydrological approach using the NWP chain driven by ECMWF (upper panels) and GFS (lower panels), for different MOLOCH horizontal resolutions. X-axis: return period T. Y-axis: probability of exceeding the return period in at least one basin within the considered region. The red vertical line indicates the maximum observed T.